*diversity*

MDPI

*Article*

# A Description of the New Hybodont Shark Genus, *Columnaodus*, from the Burlington and Keokuk Limestones (Carboniferous, Mississippian, Osagean) of Illinois and Iowa, USA

**David Cicimurri [1], Charles Ciampaglio [2,*], Matthew Hoenig [2], Ryan Shell [3], Lauren Fuelling [2], David Peterman [4], Daniel A. Cline [2] and Stephen Jacquemin [2]**

[1] South Carolina State Museum, 301 Gervais Street, Columbia, SC 29201, USA; dave.cicimurri@scmuseum.org
[2] Science, Mathematics, and Engineering Academic Unit, Wright State University Lake Campus, Celina, OH 45822, USA; hoenig2@wright.edu (M.H.); cline.74@wright.edu (D.A.C.); stephen.jacquemin@wright.edu (S.J.)
[3] Department of Vertebrate Paleontology, Cincinnati Museum Center, Cincinnati, OH 45203, USA; shell.24@wright.edu
[4] Department of Mechanical Engineering, Penn State, University Park, PA 16801, USA; david.peterman@psu.edu
* Correspondence: chuck.ciampaglio@wright.edu

**Abstract:** Bonebeds occurring in exposures of the Burlington and Keokuk Limestones (Mississippian/Osagean) along the Iowa and Illinois border (USA) contain an abundant and diverse collection of chondrichthyan remains that includes teeth, spines, denticles, and coprolites. These remains represent cochliodont, hybodont, petalodont, ctenacanthid, symmoriid, and acanthodian (stem chondrichthyan) taxa. The thickest of these beds, herein referred to as the Burlington–Keokuk bonebed, occurs at the top of the Burlington Limestone and presents a remarkable opportunity to study the assemblage of mid-continent, Middle Mississippian chondrichthyans. Bulk matrix samples of this bonebed were collected from two quarries (Biggsville Quarry, Biggsville, IL, USA, and Nelson Quarry, Mediapolis, IA, USA) and disaggregated. Among the multitude of previously known taxa, several teeth represented a new genus and species of hybodont shark. Herein, we describe these teeth as *Columnaodus witzkei* (gen. et sp. nov.), a hybodontiform with dental features comparable to unnamed specimens reported from elsewhere.

**Keywords:** hybodont; Hybodontiformes; Burlington–Keokuk; carboniferous; *Columnaodus witzkei*



**Citation:** Cicimurri, D.; Ciampaglio, C.; Hoenig, M.; Shell, R.; Fuelling, L.; Peterman, D.; Cline, D.A.; Jacquemin, S. A Description of the New Hybodont Shark Genus, *Columnaodus*, from the Burlington and Keokuk Limestones (Carboniferous, Mississippian, Osagean) of Illinois and Iowa, USA. *Diversity* **2024**, *16*, 276. https://doi.org/10.3390/d16050276

Academic Editor: Eric Buffetaut

Received: 22 February 2024
Revised: 2 May 2024
Accepted: 2 May 2024
Published: 6 May 2024



## 1. Introduction

The Burlington and Keokuk Limestones (Mississippian, Osagean) of the North American midcontinent are best known for their abundant and diverse invertebrate assemblages containing crinoids, brachiopods, and other marine invertebrates. However, the units also contain abundant vertebrate fossil assemblages, including the teeth, spines, and denticles of chondrichthyans, the teeth and scales of bony fish, the remains of acanthodians (stem chondrichthyans), and coprolites [1]. These fossils occur within thin, concentrated horizons of the Burlington Limestone and the overlying Keokuk Limestone that vary in lateral extent from tens of meters to over one hundred kilometers [1–4]. The largest of these bonebeds, the regionally continuous and laterally extensive Burlington–Keokuk bonebed, as referred to herein, is located at the top of the Burlington Limestone, at the point of contact with the Keokuk Limestone, cropping out near their type sections along the Iowa–Illinois border (Figure 1a) [1]. The Burlington–Keokuk bonebed is easily distinguishable and contains abundant vertebrate remains. Therefore, this unit presents an excellent opportunity to investigate the Osagean chondrichthyan community on the Burlington continental shelf (see Figure 2b).

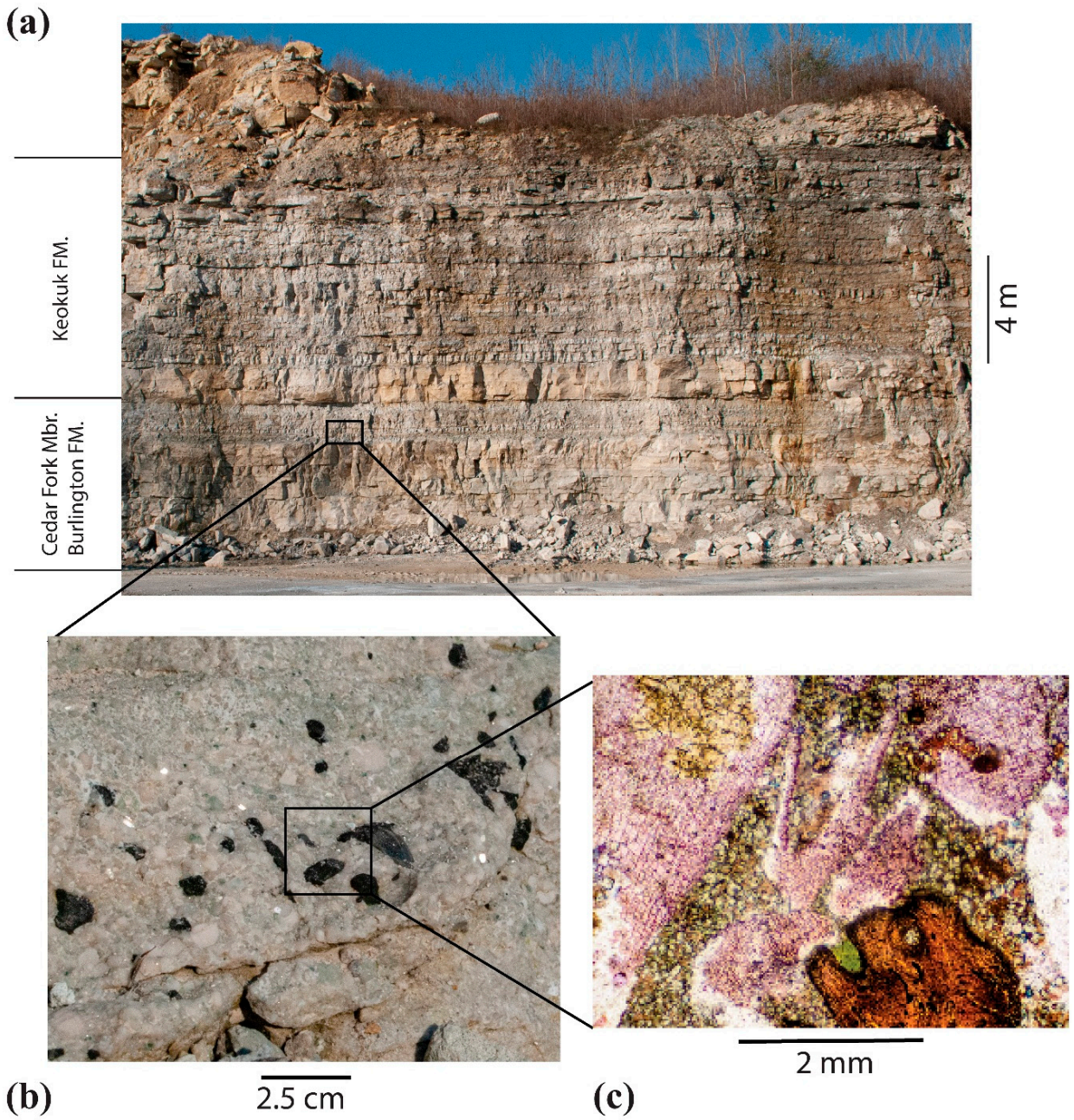


**Figure 1.** (**a**) Quarry wall at the Cessford Construction Biggsville Quarry (Illinois) showing the Burlington and Keokuk Limestones, with the stratigraphic position of the Burlington–Keokuk bonebed highlighted within the rectangle. (**b**) Field photograph showing a closeup of the Burlington–Keokuk bonebed. (**c**) Stained, thin section of the bonebed seen through transmitted light. The dark brown object in the lower right corner of panel (**c**) is an elasmobranch tooth.

Our understanding of the chondrichthyan fauna from the Burlington and Keokuk Limestones has improved significantly over the years. Early workers [2,5–12] described over 100 species of chondrichthyans from these units based on teeth, spines, and scales. However, this number has been reduced due to taxonomic revisions, missing type specimens, uninformative original descriptions, and/or illustrations lacking sufficient detail [13].

Hybodont sharks of the Burlington and Keokuk Limestones are understudied compared to other chondrichthyan groups from these units [14]. Hybodonts can be characterized as durophagous based on their teeth, although clutching/tearing and piercing dentitions were perhaps more common during the Mesozoic Era [13,15]. Additionally,

hybodont dentitions exhibit heterodonty, often disjunct, which complicates our understanding of this group's taxonomy, functional morphology, biogeography, and paleoecology. Furthermore, the generally small tooth sizes of Paleozoic hybodont taxa often result in a collecting bias, leading to them being overlooked in paleofauna. These complications warranted our reevaluation of the vertebrate fossils in the Burlington and Keokuk Limestones. The purpose of this report is to document the discovery of a new hybodont taxon that was recovered from two sites in the midcontinent USA (Figure 2a,b). Additionally, we discuss the higher taxonomic placement of the new taxon, describe the apparent heterodonty based on the isolated teeth, and note the possible paleobiogeographic distribution of the taxon.

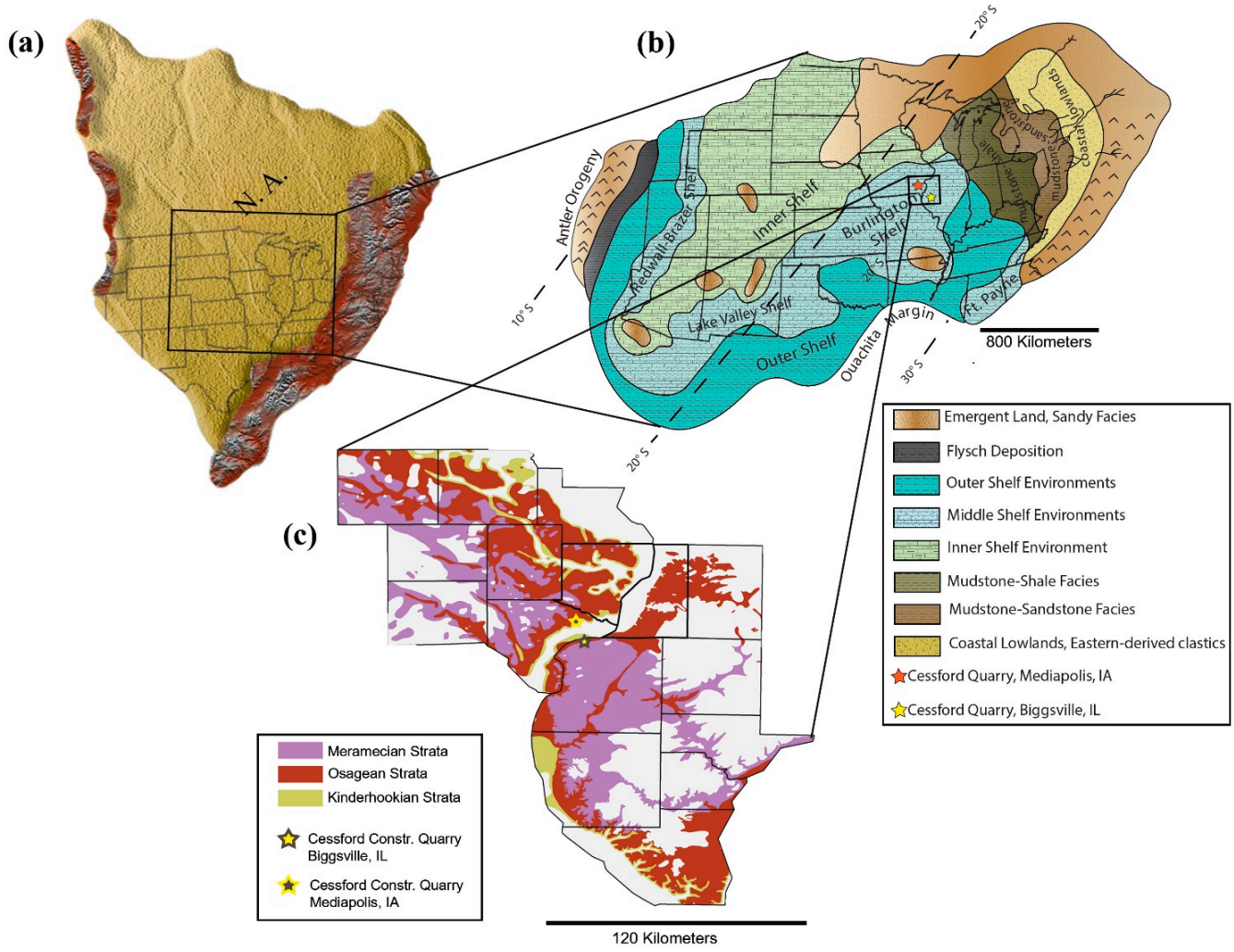


**Figure 2.** (**a**). Paleogeographic map showing the orientation of North America during the Osagean sub-epoch and the outlines of the present-day states of the USA. (**b**). Paleoenvironmental map of the area highlighted in (**a**) showing the outlines of present-day states of the USA and the locations of the study sites. (**c**). Geologic map of the area highlighted in (**b**) showing the lateral extent of Mississippian rocks and locations of the study sites (county boundaries are solid black lines).

## 2. Materials and Methods

### *2.1. Geological Setting*

#### 2.1.1. General Stratigraphy and Lithology

At the stratotype section in Burlington, Iowa, the Burlington Limestone unconformably overlies the Kinderhookian Wassonville Formation and is conformably overlain by the Keokuk Limestone [1]. The Burlington Limestone is divided into three members that, in ascending order, include Dolbee Creek, Haight Creek, and Cedar Fork (Figure 3) [1,16].

The Burlington–Keokuk bonebed occurs at the top of the Cedar Fork Member, concentrated at an abrupt but conformable contact with the Keokuk Limestone (Figures 2b and 3a) [1,16]. The clasts within the bonebed are evenly distributed and range in size from 2.5 cm to smaller than 0.5 mm. The Burlington Limestone, Keokuk Limestone, and Warsaw Shale together comprise the lithostratigraphic Augusta Group [1].

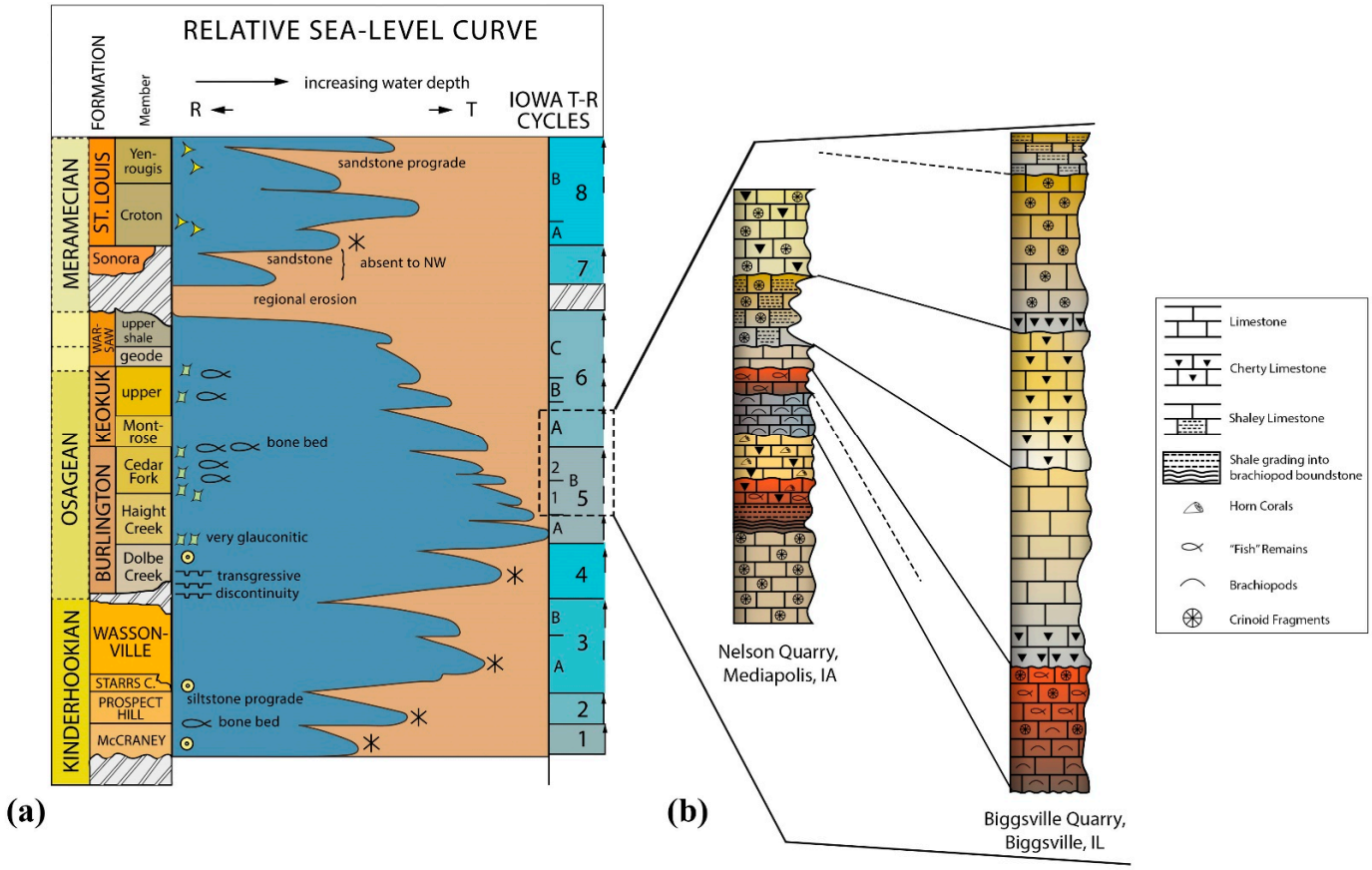


**Figure 3.** (**a**) Stratigraphic section of Mississippian strata of western Illinois and eastern Iowa placing the lithostratigraphic units in the context of transgressive and regressive episodes. (**b**) Stratigraphic sections of the Cessford Construction quarries discussed herein showing regional correlations of the units. Numbers and sub-letters in the far-right column of (**a**) represent the eight Mississippian transgressive/regressive cycles that have been identified in Iowa (i.e., the Burlington–Keokuk bonebed discussed herein marks the boundary between Cycles 5B and 6A. Dashed lines in (**b**) represent undetermined correlations of unconformities observed at the quarries.

The Burlington Limestone within southeast Iowa and northwest Illinois is lithologically complex, with strata that vary laterally (Figure 2c), even within the confines of a single quarry. The typical thickness of the Burlington Limestone in the study area ranges between 16 m and 24 m, thickening westward in the subsurface. This formation consists predominantly of crinoidal packstones and grainstones, and its various members often contain cherty, dolomitic, and glauconitic horizons [1,16].

### 2.1.2. Age and Depositional Setting

The Burlington Limestone comprises part of the Osagean-type section and is therefore of Osagean (early-middle Mississippian) age [1]. This age has been corroborated by the Osagean conodont fauna that includes *Pseudopolygnathus multistriatus* and *Indeodus regularis*, as well as the fusilinid foraminiferan genera *Priscella* and *Endothyra* [1,17–23].

The Osagean age roughly overlaps with the late Tournaisian and early Viséan ages of the European time scale. The Tournaisian–Viséan boundary (346.7 ± 0.4 ma) [24]

therefore occurs within the type Osagean, but the exact position of this boundary remains uncertain [1]. Studies of calcareous foraminifera from the Cedar Fork Member have restricted its age to no older than the late Tournaisian, but an early Viséan upper age estimate cannot be ruled out [1].

The Burlington Limestone was deposited on a carbonate ramp in the Illinois Basin, which was paleogeographically situated south of the equator, off the subtropical western Laurussian coast (Figure 2a) [20,25,26]. This lithostratigraphic unit accumulated within an inner shelf environment that was part of the broader basin (Figure 2b) [20].

#### 2.1.3. Bonebed Deposition

The Burlington and Keokuk Limestones were deposited during several transgression–regression (T-R) cycles. The Dolbee Creek and Cedar Fork members of the Burlington Limestone formed during Iowa T-R Cycle 5, and the overlying Keokuk Limestone accumulated during Iowa T-R Cycle 6 [4] (Figure 1). Some authors have asserted that the boundary between these two cycles is marked by a period of subaerial exposure [20,27], but others have contested this assertion [1,28], even going so far as to state that "absolutely no evidence" exists for subaerial exposure [16,29]. Rather, the boundary between these limestones (i.e., the Burlington–Keokuk bonebed) represents a condensed section formed during the initial transgression of Iowa T-R Cycle 6 (Figure 1), evidence for which can be found in the bonebed's abundant vertebrate remains and glauconite and its geochemistry, all of which indicate decreased sedimentation rates [4,30,31]. The condensed section hypothesis contrasts with previous explanations for bonebed formation that posited a mass fish death [3] or a "superabundant development of ichthyic life" [2].

Although most condensed beds (such as bonebeds and shell beds) accumulate in low-energy, offshore marine environments, they may still experience physical erosion and abrasion, which usually occurs via deep storm waves or bottom-flowing currents [32–35]. This most likely explains the range of preservation observed among the chondrichthyan remains within the bonebeds, which ranges from pristine to partial specimens with fully abraded surfaces. These latter specimens indicate long periods of exposure to erosional processes. Teeth of durophagous sharks tend to be better preserved than those of piscivorous taxa (due to their more compact nature and general lack of delicate features), and the preservation of smaller specimens (~<1 cm) is generally better than that of larger specimens. However, many of the fossils we describe below are heavily weathered, indicating the long-term exposure of the substrate.

### *2.2. Material Collection and Preparation*

#### 2.2.1. Sample Locations

To expand on the limited historical survey data that are available for the bonebed, samples of the Burlington–Keokuk bonebed were collected both in situ and ex situ (float from spoil piles). Several trips to the Nelson and Biggsville Quarries (Figures 1a, 2b and 3b), both operated by Cessford Construction Company (Ogden, UT, USA), were undertaken between 2008 and 2009.

#### 2.2.2. Laboratory Processing

Hand tools and powered rock saws were used for rock extraction. Intact teeth exposed on rock surfaces were prepared with pneumatic tools. Limestone was broken into fragments roughly 2 cm in dimension with a pneumatic rock splitter and dissolved using standard methods for carbonate dissolution [36–38]. The Biggsville rock sample was dissolved using a solution of 10% formic acid with additional calcium carbonate, whereas the Mediapolis material was dissolved using a 10% acetic acid solution with calcium carbonate. The samples were dissolved with different acids as part of another project on carbonate acid dissolution. The type of acid used did not affect the quality of vertebrate remains obtained from the limestones. The resulting slurries were washed and sieved using #4, #10, #20, #40, #60, and #80 Tyler USA Standard Soil sieves, and particles larger than 5 mm to as small as

250 µm were recovered. The resulting concentrates were then sorted under Amscope stereo microscopes and vertebrate fossils were removed using damp paint brushes. Photographs of the hybodont teeth described herein were obtained by a digital image-stacking process. This process involved using an infinity-corrected macro lens and a macro extension tube lens affixed to the front of a Nikon D7100 digital SLR. This whole apparatus was attached to a StackShot macro rail, allowing multiple photographs to be taken with fixed focal planes. The macro rail decreased the distance between the lens and the subject at fixed intervals, which was set to the width of the focal plane. The resulting photos were then stacked digitally using the software Helicon Focus (www.heliconsoft.com), which removed out-of-focus portions, creating a photomosaic. This process produces small-scale images with true color and high focus across the entire topology of a surface.

#### 2.2.3. Repository, Taxonomy, and Terminology

The specimens described herein are housed at the South Carolina State Museum in Columbia (SC) and are curated under accessions SC2019.44 and SC2022.35. Taxonomic rankings and descriptive terminology largely follow Ginter et al., 2010 [13]. A species occurrence list is included in the Supplementary Information section.

## 3. Results

### *3.1. Bonebed Lithology*

The lithology of the Burlington–Keokuk bonebed varies from location to location. Thin sections revealed that at Nelson Quarry (Mediapolis, IA, USA), it is primarily a crinoidal wackestone with approximately 10–15% vertebrate remains and phosphatic pellets and granules by volume. The original lime mud has been replaced mainly with nonplanar dolomite and occasional euhedral dolomite (Figure 3a). At the Biggsville Quarry (Biggsville, IL, USA), the bonebed is primarily a crinoidal wackestone with approximately 5–10% vertebrate remains and phosphatic pellet granules. The original lime mud has been replaced mainly with euhedral dolomite (Figure 1c). The bonebeds at both localities contain locally abundant amounts of glauconite granules.

### *3.2. Systematic Paleontology*

- Class Chondrichthyes Huxley, 1880 [39]
- Subclass Elasmobranchii Bonaparte, 1838 [40]
- Infraclass Euselachii Hay, 1902 [41]
- Order Hybodontiformes Maisey, 1975 [42]
- Superfamily Hybodontoidea Owen, 1846 [43]
- Family incertae sedis
- Genus *Columnaodus* gen. nov.
- urn:lsid: zoobank.org:act:BB92D0D8-66EE-45CE-B5F2-8FDEE2DE9EB7

#### 3.2.1. Diagnosis

Generic diagnosis: Genus of durophagous hybodont shark characterized by presumed anterior teeth having a trilobed occlusal outline and mesio-distally wide but labio-lingually thin lateral teeth. Anterior teeth bear a robust medial cusp and one pair of lateral cusplets, whereas lateral teeth typically bear a small medial cusp and one to two pairs of very diminutive lateral cusplets. The labial and lingual crown faces are prominently convex in the areas of the medial cusplet and lateral cusplets. Additionally, teeth exhibit a prominent labial peg. The medial and lateral cusplets are generally connected by a transverse ridge, and additional, much shorter ridges may emanate from the cusp and/or cusplet apices. The tooth base is very high (apico-basally), averaging 63% of total tooth height (minimum 50%, maximum 75%). The base is also nearly as wide (mesio-distally) or even slightly wider than the crown, and it is labio-lingually thin, generally being one-half as wide as the crown. Furthermore, the base is highly vascularized, with a row of foramina occurring below the

labial and/or lingual crown foot, as well as scattered throughout the surface of one or both faces and often the aboral surface.

1. Columnaodus witzkei sp. nov.
2. Figures 4–6

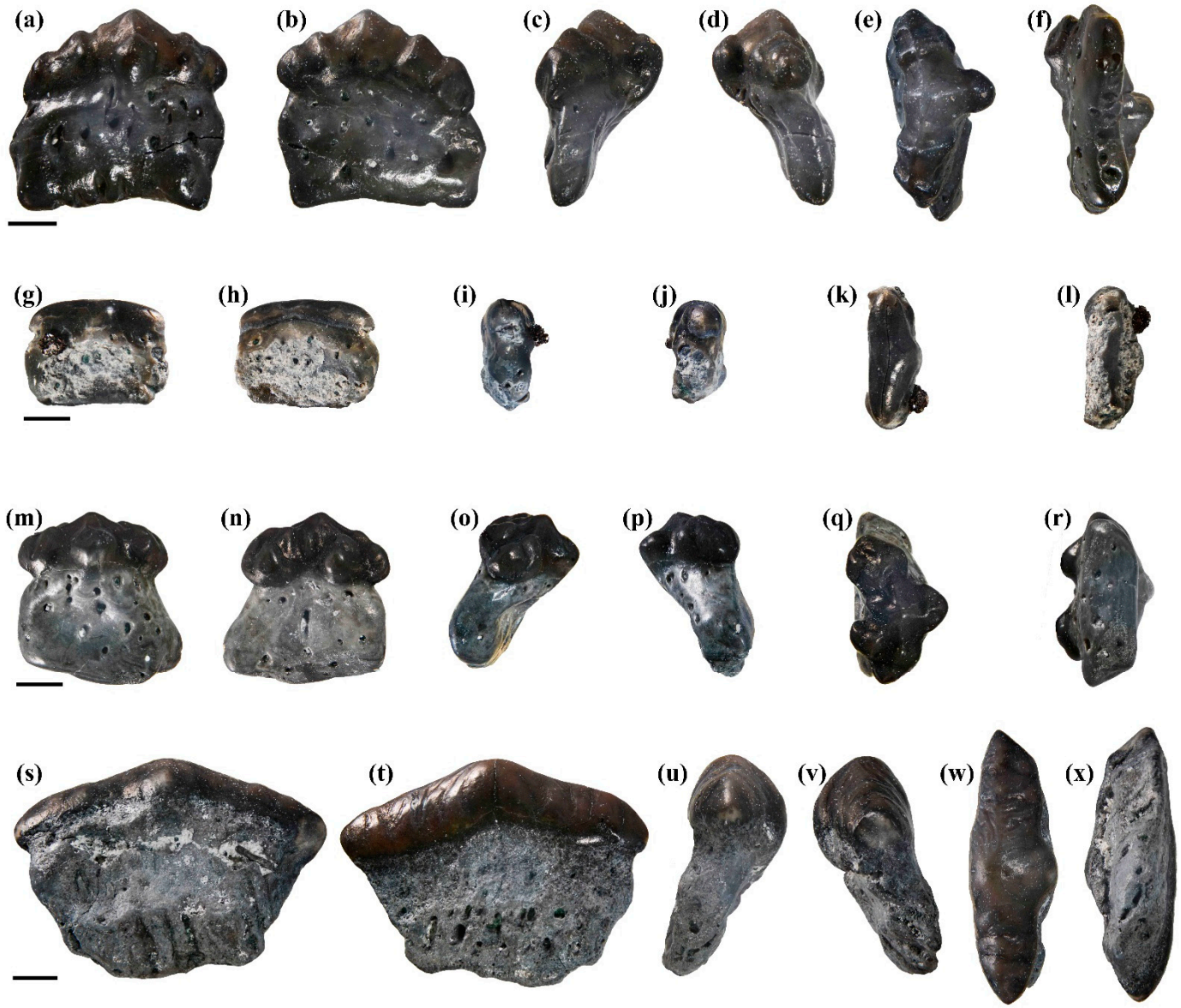


**Figure 4.** Teeth of *Columnaodus witzkei* gen. et sp. nov. comprising the hypodigm. (**a**–**f**) Holotype, SC2019.44.1. (**a**) Labial, (**b**) lingual, (**c**) mesial?, (**d**) distal?, (**e**) occlusal, (**f**) basal views. (**g**–**l**) Paratype, SC2022.35.3. (**g**) Labial, (**h**) lingual, (**i**) mesial?, (**j**) distal?, (**k**) occlusal, (**l**) basal views. (**m**–**r**) Paratype, SC2022.35.4. (**m**) Labial, (**n**) lingual, (**o**) distal?, (**p**) mesial?, (**q**) occlusal, (**r**) basal views. (**s**–**x**) Paratype, SC2022.35.9. (**s**) Labial, (**t**) lingual, (**u**) mesial?, (**v**) distal?, (**w**) occlusal, (**x**) basal views. Labial at right in (**c**,**e**,**f**,**i**,**k**,**l**,**o**,**q**,**r**,**u**,**w**); labial at left in (**d**,**j**,**p**,**v**,**x**). Scale bars = 1 mm for all.

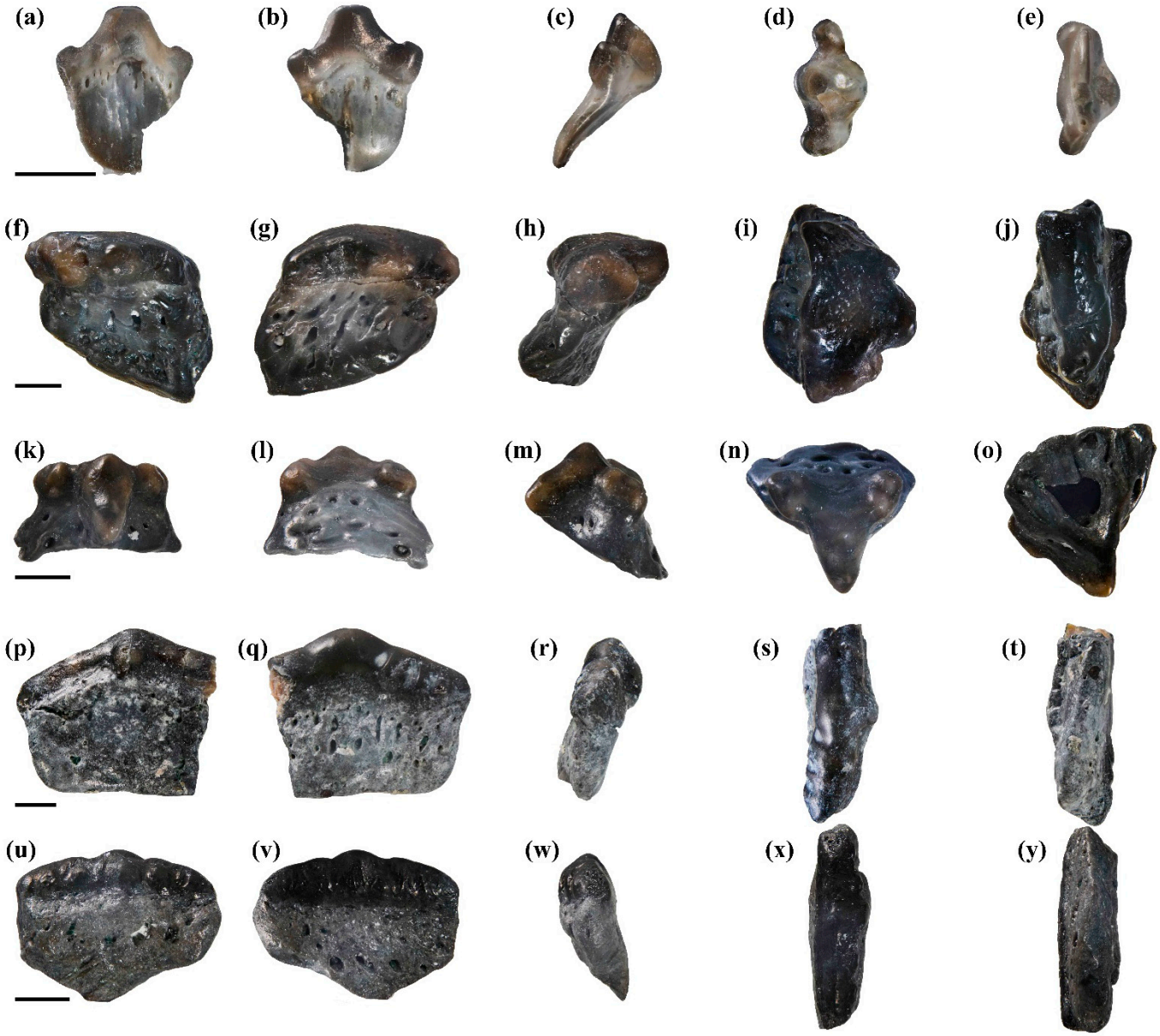


**Figure 5.** *Columnaodus witzkei* gen. et sp. nov. teeth. (**a**–**e**) SC2022.35.1. (**a**) Labial, (**b**) lingual, (**c**) profile, (**d**) oral, (**e**) aboral views. (**f**–**j**) SC2022.35.2. (**f**) Labial, (**g**) lingual, (**h**) profile, (**i**) oral, (**j**) aboral views. (**k**–**o**) SC2022.35.8. (**k**) Labial, (**l**) lingual, (**m**) profile, (**n**) oral, (**o**) aboral views. (**p**–**t**) SC2022.35.7. (**p**) Labial, (**q**) lingual, (**r**) profile, (**s**) oral, (**t**) aboral views. (**u**–**y**) SC2022.35.6. (**u**) Labial, (**v**) lingual, (**w**) profile, (**x**) oral, (**y**) aboral views. Labial at right in (**c**–**e**,**h**,**i**,**r**,**s**,**x**); labial at left in (**j**,**m**,**w**); labial at bottom in (**n**,**o**). Scale bars = 1 mm for all.

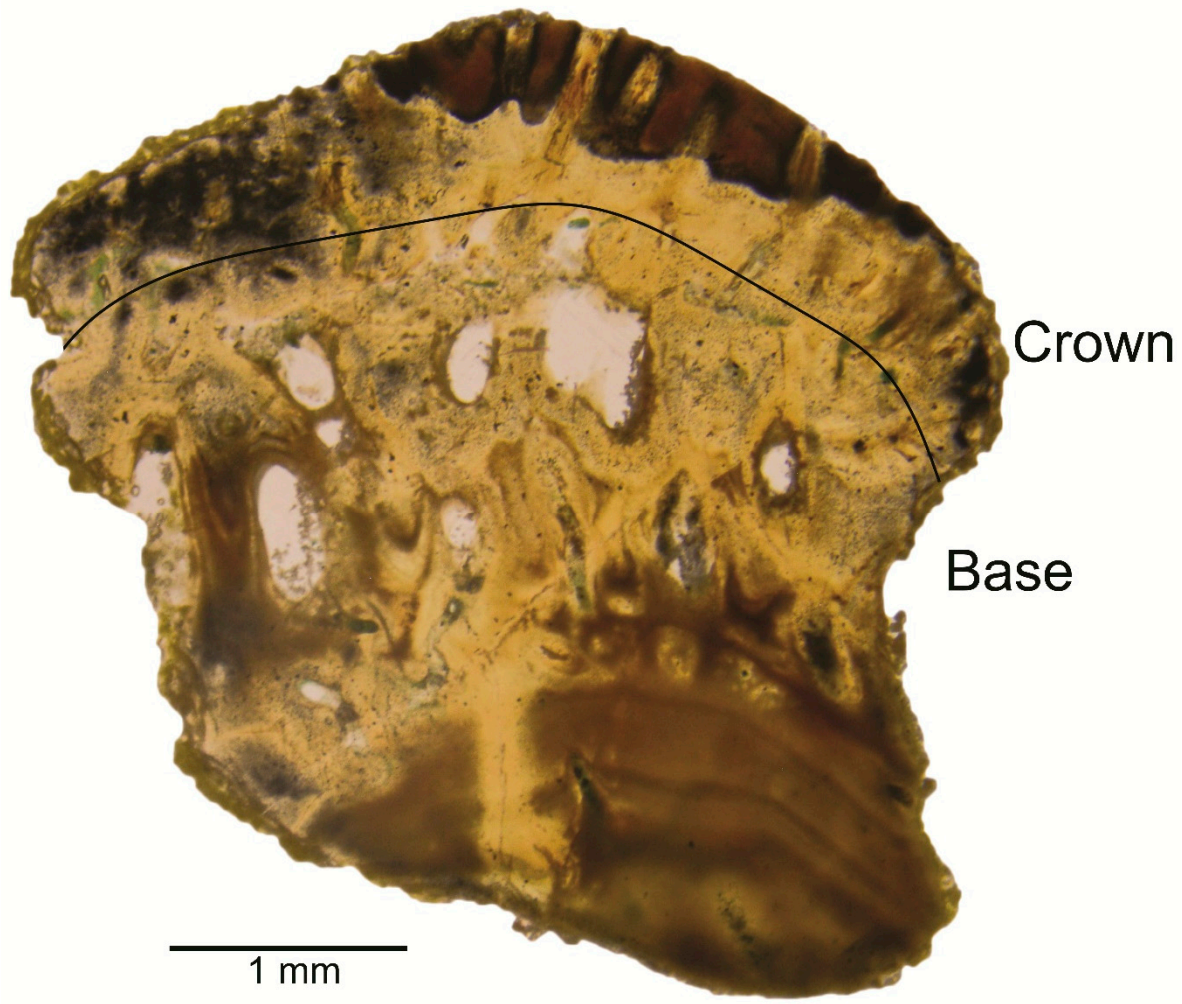


**Figure 6.** Thin section of a *Columnaodus witzkei* gen. et sp. nov. tooth (SC2022.35.10) under transmitted light. Curved solid line indicates the approximate trend of the crown foot.

3. urn:lsid:zoobank.org:act:09075140-9525-4461-BFCD-F3D54A9F802E

- Species diagnosis: as for the genus.
- Hypodigm: holotype, SC2019.44.1 (Figure 4a–f); paratype, SC2022.35.3 (Figure 4g–l); paratype, SC2022.35.4 (Figure 4m–r); paratype, SC2022.35.9 (Figure 4s–x).
- Additional specimens examined: SC2019.44.2, SC2019.44.3, SC2019.44.4, SC2019.44.5, SC2019.44.6, SC2022.35.1 (Figure 5a–e), SC2022.35.2 (Figure 5f–j), SC2022.35.5, SC2022.35.6 (Figure 5u–y), SC2022.35.7 (Figure 5p–t), SC2022.35.8 (Figure 5k–o).
- Stratigraphic occurrence and age: Burlington–Keokuk bonebed, contact horizon between Burlington and Keokuk Limestones (Figures 1a and 3b); Illinois and Iowa, USA (Figure 2b); Carboniferous Period, Mississippian Subperiod, Osagean sub-epoch (Tournasian to Viséan stages).
- Type locality: Cessford Construction Company Mediapolis Quarry, Mediapolis, Des Moines County, Iowa, 41.00997, −91.05281 (Figure 2b).

3.2.2. Etymology

The genus name *Columnaodus* is derived from the combination of the Latin words "columna", meaning column, and "odus", for tooth. The name is suggested due to the high, narrow, column-like tooth profile, as well as the crown ornamentation that resembles columnal fluting. The specific epithet *witzkei* recognizes the outstanding efforts of Dr. Brian

Witzke for his decades-long study of the geology of Iowa in general, and Mississippian strata in particular.

#### 3.2.3. Description

Specimen SC2019.44.1 is designated as the holotype (Figure 4a–f). The tooth consists of a crown and well-differentiated base. Total tooth height measures roughly 4.3 mm, with the base constituting 65% of this value (2.8 mm at greatest height). The crown is low, and meso-distally wide, measuring 4.5 mm in this dimension. The crown includes a broad but low, pointed medial cusp that is slightly distally directed and flanked by mesial and distal shoulders (aka "wings"). The mesial shoulder is more elongated than the distal shoulder and is also more oblique to cusp height, and this morphology results in a concave crown foot. Both shoulders bear two indistinct cusplets that decrease in size distally, with those on the mesial side being slightly more conspicuous than those on the distal side (Figure 4a,b). The shoulders continue a short distance beyond the secondary cusplets and terminate at rounded margins. A pronounced peg (aka protuberance) occurs at the crown foot below the medial cusp (Figure 4a). Overall, the labial and lingual crown faces are convex, but the faces are particularly convex in the areas of the lateral cusplets. In oral view, the lateral shoulders are somewhat lingually curving; the medial cusp and lateral cusplets are connected by a conspicuous, smooth transverse ridge; and a robust ridge extends from the main cusp apex onto the apical surface of the labial peg (Figure 4e). In labial and lingual views, the mesial side of the tooth base is lower than the distal side due to the oblique trend of the mesial crown shoulder and the mesial side extends beyond the crown. In profile views (Figure 4c,d), the tooth base thins aborally, the labial surface is concave, and the lingual surface is convex. Numerous foramina occur in a row within a constricted portion of the base located just below the labial crown foot, and several foramina are more randomly scattered on the labial and lingual faces (Figure 4a,b). A row of additional foramina occurs on the very narrow aboral surface (Figure 4f).

Tooth SC2019.44.2 (not illustrated) is a small tooth measuring 2 mm in total width and roughly 1.5 mm in total height. The tooth base itself measures 1 mm in height (66% of total tooth height), but the occlusal surface of the crown is highly abraded and its original height is unknown. In labial and lingual views, the crown foot is thin, rather straight, and slightly overhangs the base. In occlusal view, the crown margins are irregular. The labial face of the tooth base lacks foramina, but a few foramina are scattered on the lingual face. In profile view, the thin base is lingually directed.

Specimens SC2019.44.3, SC2019.44.4, and SC2019.44.6 (none illustrated) are morphologically similar to each other. These abraded specimens measure 2 mm, 3 mm, and 2.2 mm, respectively, in total width and 1.9 mm, 2.1 mm, and 2 mm, respectively, in total height. In labial and lingual views, the low crowns (1 mm or less in height) are roughly symmetrical, with a very small, short, rounded medial cusp flanked by elongated lateral shoulders of nearly equal length. The labial and lingual crown foot of SC2019.44.3 is rather straight because the shoulders are perpendicular to the crown height. In contrast, the obliquely oriented shoulders of SC2019.44.4 and SC209.44.6 produce a concave labial crown foot. In all cases, the labial crown foot overhangs the root. In occlusal views, the abraded crowns are clearly divided into a rather narrow and flat lingual face and a larger, more convex labial face. In profile view, the thin base is lingually directed. Several labial and/or lingual foramina occur in a row just below the crown foot.

SC2019.44.5 is a small tooth measuring 2 mm in width and 2 mm in total height. The crown is low in labial/lingual views, with a straight occlusal surface and crown foot. In occlusal view, the crown is triangular. The labial and lingual crown foot are thickened, but the labial face also bears a massive medially located peg. In profile view, this peg extends well beyond the tooth base. The base constitutes most of the total tooth height. In profile view, it is labio-lingually thin and lingually directed. The labial face is concave and nutritive foramina occur immediately below the crown foot, adjacent to the labial peg. Additional foramina are located below the lingual crown foot.

Specimens SC2022.35.1 (Figure 5a–e), SC2022.35.4 (paratype; Figure 4m–r), and SC2022.35.8 (Figure 5k–o) are of comparable morphology. SC2022.35.1 measures 2 mm in preserved height (the main cusp apex is incomplete) and the crown is 1.8 mm wide. Specimen SC2022.35.4 is 4.5 mm high and the crown of SC2022.35.8 is 3.1 mm high and measures 3 mm in width. All these specimens include a crown that has a trilobed outline in occlusal view, with a labial peg flanked by a robust lateral cusplet occurring on a short lateral shoulder, which is oblique to the axis of the projection (Figures 4q and 5d,n). There is a medial cusp that is very broad basally and varies in height (compare Figures 4n and 5b,l). The lateral cusplets are low (apparently broken on SC2022.35.1), pointed, broadly conical, and may be diverging from the main cusp (Figures 4m and 5a,k). In lingual view, the crown foot of each specimen is concave. SC2022.35.1 is ablated, but SC2022.35.4 and SC2022.35.8 preserve short ridges that emanate from the middle of the medial cusp. On SC2022.35.4, the ridges extend onto the labial peg and lateral shoulders (Figure 4q), but they only extend onto the lateral shoulders on SC2022.35.8 (Figure 5n). Additionally, the ridges of SC2022.35.4 bifurcate distally, and there are supplemental short ridges on a lateral prong that form cusplet-like structures. The tooth base is generally high, comprising more than 67% of the total height of SC2022.35.4, and it is wider (mesio-distally) than the crown on SC2022.35.4 and SC2022.35.8. The labial and lingual faces of the tooth base of SC2022.35.4 (Figure 4m,n) and SC2022.35.8 (Figure 5k,l) are perforated by numerous large foramina. On SC2022.35.1, foramina occur in a row below the crown foot on the labial and lingual faces (Figure 5a,b). The width of the base on these specimens is variable, with that of SC2022.35.1 being narrower than the crown (although broken, but see Figure 5a), whereas that of SC2022.35.4 is well short of the crown margin on one side but extends well beyond it on the other side (Figure 4m). The base of SC2022.35.8 protrudes laterally beyond both lateral crown margins (i.e., Figure 5k). In profile views, the tooth bases of SC2022.35.1 and SC2022.35.4 are lingually directed and labio-lingually thinner than the crown (compare Figures 4o and 5c). The aboral surfaces of these bases are thin to wide, with that of SC2022.35.4 bearing several foramina (Figures 4r and 5e).

Tooth SC2022.35.2 (Figure 5f–j) is somewhat similar to the aforementioned specimens. It measures 3.7 mm in maximum height and the crown is 3.9 mm wide, with the base constituting up to 67% of the total tooth height. In labial and lingual views, the crown is very low with an almost flat occlusal surface (Figure 5f,g). In occlusal view, the crown is thick (labio-lingually) with a pitted surface. The lingual margin is sinuous, whereas the labial margin is dominated by a massive medial peg that is flanked by much smaller lateral protuberances (Figure 5i). In profile view, the low, flat crown is clearly delineated from the base but has a constriction, and the base is seen to be thinner than the crown and also lingually directed (Figure 5h). The labial and lingual faces of the tooth base bear numerous large foramina (Figure 5f,g). The thin, aboral surface of the base is perforated by several foramina (Figure 5j).

Specimen SC2022.35.6 (Figure 5u–y) measures 3 mm in preserved height (the root is damaged) and the crown is 4.1 mm wide. The tooth base constitutes more than 70% of the total tooth height. The tooth crown consists of a low and convex medial cusp flanked by elongated lateral shoulders. The mesial shoulder is slightly more elongated than the distal one and, overall, the crown is straight (Figure 5u,v). The medial cusp is somewhat separated from the lateral shoulders by a shallow and rounded notch, with the shoulder immediately adjacent to the notch having a cuspidate appearance (Figure 5u). As is the case on SC2022.35.7 and SC2022.35.9, there are conspicuous labial and lingual swellings on the crown (Figure 5u,v). There is a weak labial peg at the base of the medial cusp (Figure 5u). There are minute, chevron-shaped ridges along the crown foot of the labial and lingual faces (Figure 5u,v). In profile view, the crown is convex labially but rather flat lingually and the tooth base is sharply tapering aborally (Figure 5w). In occlusal view, the crown is divided into a more expansive labial face and a relatively thin lingual face by a conspicuous transverse crest (Figure 5x). The lingual face of the tooth base is perforated by several

large foramina (Figure 5v), and there are fewer foramina on the labial face (Figure 5u). The aboral margin of the tooth base is sharp (Figure 5x).

Specimen SC2022.35.7 (Figure 5p–t) is broken but was a very wide tooth. The crown measures 5 mm in width (the mesial? side is damaged), and the total tooth height is 4.5 mm, with the base constituting more than 70% of this value. The medial portion of the crown is weakly cuspidate and there is a robust, rounded labial peg (Figure 5u). Elongated oblique shoulders extend obliquely from the medial cusp and, although lateral cusplets are not obvious, there are conspicuous swellings on the labial and lingual faces (Figure 5p,q). In occlusal view, a distinct transverse crest (Figure 5s) subdivides the crown into roughly equal labial and lingual parts. In profile view, the tooth base is lingually directed and thinner than the crown (Figure 5r). The aboral surface is ablated but bears several foramina (Figure 5t). There are fewer foramina on the labial face of the tooth base compared to the lingual face (Figure 5p,q).

Specimen SC2022.35.9 (Figure 4s–x) is designated as a paratype and has a comparable morphology to SC2022.35.6 (Figure 5u–y) and particularly SC2022.35.7 (Figure 5p–t). Tooth SC2022.35.9 is the largest specimen available to us, measuring 7 mm in preserved total width and 5 mm in total height. The tooth base constitutes roughly 70% of the total tooth height. In labial view, the medial portion of the crown is weakly cuspidate and there is a robust rounded medial peg at the crown foot (Figure 4s). Elongated oblique shoulders of roughly equal length extend laterally to form the crown margins. Both shoulders possess a pair of convex areas that delineate the locations of cusplets that are barely perceptible along the occlusal margin (more easily seen in Figure 4s). In oral view, the crown is bi-convex and separated into labial and lingual faces by an indistinct transverse ridge. Additional faint rugosities are visible around the main cusp (Figure 4w). In profile views, the bi-convex crown is slightly lingually directed (Figure 4v). The tooth base is high, lingually directed, labio-lingually thin, and tapers aborally (Figure 4u). The labial and lingual faces are perforated by numerous very small foramina, and the lower one-half of the lingual face bears several larger foramina (Figure 4s,t). The aboral surface of the base also bears several foramina (Figure 4x). The base appears to be less wide than the crown (i.e., Figure 4t), but this is partly an artifact of preservation.

SC2022.35.3 is a paratype specimen (Figure 4g–l). This small tooth measures 2 mm in height, the crown is 3.5 mm wide, and the base represents over 70% of the total tooth height. The specimen has a wide, straight, low, featureless crown. In profile view, the crown is thick (labio-lingually) and the occlusal surface is convex (Figure 4i,j). The only identifying feature is a short and rounded labial peg (Figure 4g). In occlusal view, the crown is convex and the labial peg is wide but short (Figure 4k). The base is high and extends slightly beyond the lateral crown margins (Figure 4h); it is labio-lingually thin (Figure 4i,j) and perforated on both sides by numerous foramina (Figure 4g,h). The aboral surface is narrow (Figure 4l). Specimen SC2022.35.5 (not illustrated) is a broken and ablated tooth measuring 2 mm in height and 2.3 mm in crown width as preserved (crown margins are damaged). It is comparable to SC2022.35.3 but the labial peg is more conspicuous. Additionally, there is a conspicuous row of foramina on the lingual surface of the tooth base, just below the crown foot.

#### 3.2.4. Remarks

A thin section was made of a *Columnaodus* gen. nov. tooth (SC2022.35.10) and transmitted light revealed the tooth histology (Figure 6). Based upon our observations and comparisons to thin sections shown in the literature [13,44], the new taxon described herein resides within the Hybodontiformes. The teeth lack tubules within the crown, which may exclude placement in the family Acrodontidae [13,45]. If the genus *Polyacrodus* is treated as a *nomen dubium* (consisting of species more appropriately assigned to other hybodontid genera), the validity of the family Polyacrodontidae (which currently also includes *Roongodus*) can be called into question and is therefore not considered herein [46–48]. Furthermore, the tooth shape, including the crown and base, eliminates consideration of the

currently monogeneric family Tristychiidae [49]. Of the two remaining accepted families, the Hybodontidae is considered strictly a Mesozoic taxon [13]. However, there are taxa within this family with teeth comparable to *Columnaodus* gen. nov., but those species lack a labial crown peg and the root is very short (i.e., Maisch and Matzke, 2016 [50]). The family Lonchidiidae may be appropriate for the inclusion of *Columnaodus* gen. nov. as the crown morphology and internal composition are comparable [51–54]. However, Ginter et al. [13] commented on the complications of utilizing tooth histology to determine familial placement of Paleozoic hybodonts, and we therefore refrain from assigning the new taxon to a family. In any case, the dentition of the new taxon, as interpreted herein, is somewhat different from representatives of the currently recognized Paleozoic hybodont families (see below), reinforcing our utilization of *incertae sedis* at this time.

The crown of *Columnaodus witzkei* gen. et sp. nov. bears a labial peg and the base is mesio-distally wide and highly vascularized, features shared with Paleozoic hybodont sharks within Acrodontidae [55], Lonchidiidae [56], and Polyacrodontidae [57]. We believe that the peg was labially located rather than lingually, as has been described for Paleozoic hybodonts like *Hamiltonichthys* and *Onychoselache* (i.e., Maisey, 1989 [58]; Coates and Gess, 2007 [59]) based on, as interpreted herein, the lingual inclination of the crown in profile view. The alternative, that the crown is labially inclined and the peg occurs distally, is inconsistent with our observations of other elasmobranch teeth. Although of variable morphology, all the specimens possess some or all of the features diagnosing the new taxon, and we therefore consider them to be conspecific. The variation likely reflects at least monognathic heterodonty, with specimens like SC2022.35.1 (Figure 5a–e), SC2022.35.2 (Figure 5f–j), SC2022.35.4 (Figure 4a–f), and SC2022.35.8 (Figure 5k–o) potentially representing anterior jaw positions. The mesio-distally very wide specimens, like SC2022.35.6 (Figure 5u–y), SC2022.35.7 (Figure 5p–t), and SC2022.35.9 (Figure 4s–x), are from lateral tooth files. Specimens SC2022.35.7 and SC2022.35.9 have an angular appearance in labial view, with elongated shoulders extending obliquely from the medial portion of the crown (see Figures 5q and 4t, respectively), whereas the crown of SC2022.35.6 is essentially straight (Figure 5v). This difference in gross morphology may reflect proximity to the symphysis, with the crown becoming straighter towards the commissure (i.e., SC2022.35.7 was closer to the symphysis than SC2022.35.6). Specimen SC2022.35.3 (Figure 4g–l) has a straight crown and a labial peg but it lacks a main cusp, lateral cusplets, and ridges, indicating that this tooth was located in a posterior tooth file (i.e., closest to the jaw hinge). An increase in tooth width, along with increased distal inclination and/or offset of the medial cusp, from the symphysis towards the commissure, has been documented in Paleozoic hybodont sharks [48,58–60]. Our observations of the *Columnaodus witzkei* gen. et sp. nov. teeth are consistent with those of the aforementioned reports.

Ontogenetic heterodonty also appears to have been developed in the new taxon, based on the various tooth sizes contained in our sample. For example, tooth SC2022.35.1 (Figure 4a–e) is a smaller version (1.8 mm wide) of SC2022.35.2 (4.3 mm wide; see Figure 5f–j). Additionally, SC2019.44.4, SC209.44.6, and SC2022.35.5 (not illustrated) are essentially smaller versions of SC2022.35.7 (Figure 5p–t) and SC2022.35.9 (Figure 4s–w).

As many Paleozoic and Mesozoic hybodont sharks have teeth like those of *Columnaodus* gen. nov., comparisons to the various species are warranted. The only other Paleozoic hybodont having a tooth base comparable to that of *Columnaodus witzkei* gen. et sp. nov. is *Onychoselache*, a Mississippian (Viséan) taxon of undetermined familial placement known from Scotland and possibly China [49,59,61]. However, the latter taxon is clearly distinguished by its lack of lateral cusplets and labial and lingual crown swellings, and a conspicuous crown protuberance occurs lingually. The new taxon also differs from various species of *Mesodmodus* (Family *incertae cedis*) described by St. John and Worthen (1975) [7] from Tourniasian–Viséan rocks of Iowa by the much-reduced size of the medial cusp and lateral cusplets, weaker crown ornamentation, and much higher base. The teeth of the various species currently ascribed to *Polyacrodus*, as well as those of *Roongodus*, have a much shorter tooth base and much larger medial cusp compared to *Columanodus witzkei* gen. et

sp. nov. [60,62]. The former two taxa are known from Permo-Carboniferous and Devonian strata, respectively. With respect to the genera of generically diverse Lonchidiidae, teeth of *Dubasacanthus* (Pennsylvanian Subperiod, Illinois) are only one-quarter the size of the smallest *Columnaodus witzkei* gen et sp. nov. tooth available to us, and the crown of the former lacks ornamentation and the base is shorter [63]. Teeth of *Gansuselache* from the Permian of China can be differentiated from *Columnaodus witzkei* gen. et sp. nov. by the small overall tooth size (3 mm wide versus 7 mm for the new taxon), very large medial cusp and prominent lateral cusplets (up to two pairs), conspicuous crown ridges, lower base, and lack of nutritive foramina below the crown [53]. Teeth of *Lissodus* are highly variable, but, in general, they have a shorter root that, on anterior teeth, is clearly delineated from the crown by a prominent constriction, and the aboral surface is at least nearly as wide as the crown [14,64]. Additionally, the lateral teeth of *Lonchidion* do not appear to become as large as those of *Colmnaodus witzkei* gen. et sp. nov. Teeth of Jurassic *Luopingselache* [48] are larger than those of *Columnaodus witzkei* get. et sp. nov, the medial cusp is much larger, lateral cusplets on lateral teeth are more conspicuous, crown ornamentation is very well developed, and the tooth base is much shorter. Additionally, Jurassic *Jiaodontus* [65] teeth are quite similar to those of *Lissodus*, with anterior and lateral teeth of the former having a constriction between the crown and base, and the labial peg is smaller and base shorter than as observed on *Columnaodus witzkei* gen. et sp. nov. teeth. All of these taxa within Lonchidiidae noted above are readily distinguished by their short base (less than one-half of total tooth height) and row of nutritive foramina below the labial crown foot. In contrast, teeth of *Colmnaodus witzkei* gen. et sp. nov. have a much higher base (exceeding 60% of total tooth height) and a row of nutritive foramina can occur below the labial and lingual crown foot of a tooth. Furthermore, none of the aforementioned genera appear to have possessed an anterior tooth morphology like that of *Colmnaodus witzkei* gen. et sp. nov.

Teeth that we believe represent anterior files are comparable to a tooth from the Tournaisian of southern China that was documented by Ginter and Sun, 2007 [66], as both morphologies have a roughly trilobed occlusal crown outline and high and very vascularized base. The Chinese material may be congeneric with the USA *Columnaodus* specimens, thereby extending the paleobiogeographic range to encompass the area between these two regions.

## 4. Discussion and Conclusions

*Columnaodus witzkei* gen. et sp. nov. is a hybodont shark known based on numerous teeth recovered from a bonebed occurring in the contact zone of the Burlington and (overlying) Keokuk Limestones. This Osagean taxon exhibits dental similarities to taxa within Acrodontidae, Hybodontidae, and Lonchidiidae, but significant differences that include a row of nutritive foramina below the labial and lingual crown foot, overall height of the base, and gross morphology of anterior teeth lead us to refrain from assigning the species to any particular family. The tooth shape of this new taxon is comparable to a specimen previously reported from China, and the fossils may be congeneric. If so, the paleobiogeographic of the genus would include the region between these two widely separated areas (Figure 7).

The teeth of many Paleozoic hybodont taxa are indicative of durophagous predation, and *Columnaodus witzkei* gen. et sp. nov. appears to fall within this category. *Columnaodus* teeth occur in loose association with marine invertebrates like crinoids and brachiopods, which may have been a food source for this shark. Paleozoic chondrichthyans are known to have fed upon crinoids [67], and the relative abundance of *Columnaodus* may indicate a preference for feeding on these animals and/or other shelled invertebrates. The presumed lateral (SC2022.35.9) and posterior teeth (SC2022.35.3) are elongated with convex labial and lingual faces, low and blunt cusps and lateral cusplets, and crests and other nodular structures that would, overall, allow for shell processing and even the distribution of bite stress. The larger main cusp and lateral cusplets of presumed anterior teeth (e.g., SC2022.35.1 and SC2022.35.8) may have performed a grasping function, allowing the animal to pick up prey and then crush it with lateral and posterior teeth. This combina-

tion of grasping and crushing dentition is unique among Paleozoic hybodont taxa, but reminiscent of extant *Heterodontus*. The recognition of this unusual dentition indicates a wider variation in Paleozoic hybodont tooth morphologies than previously thought. The fact that it was discovered in an otherwise well-studied region demonstrates the pitfalls of interpreting the fossil record with a sample biased towards larger material. Additional, well-preserved specimens are required to address unanswered questions related to *Columnaodus*, like its familial position, as well as the evolutionary history, paleoecology, and paleobiogeography of hybodontiforms in general.

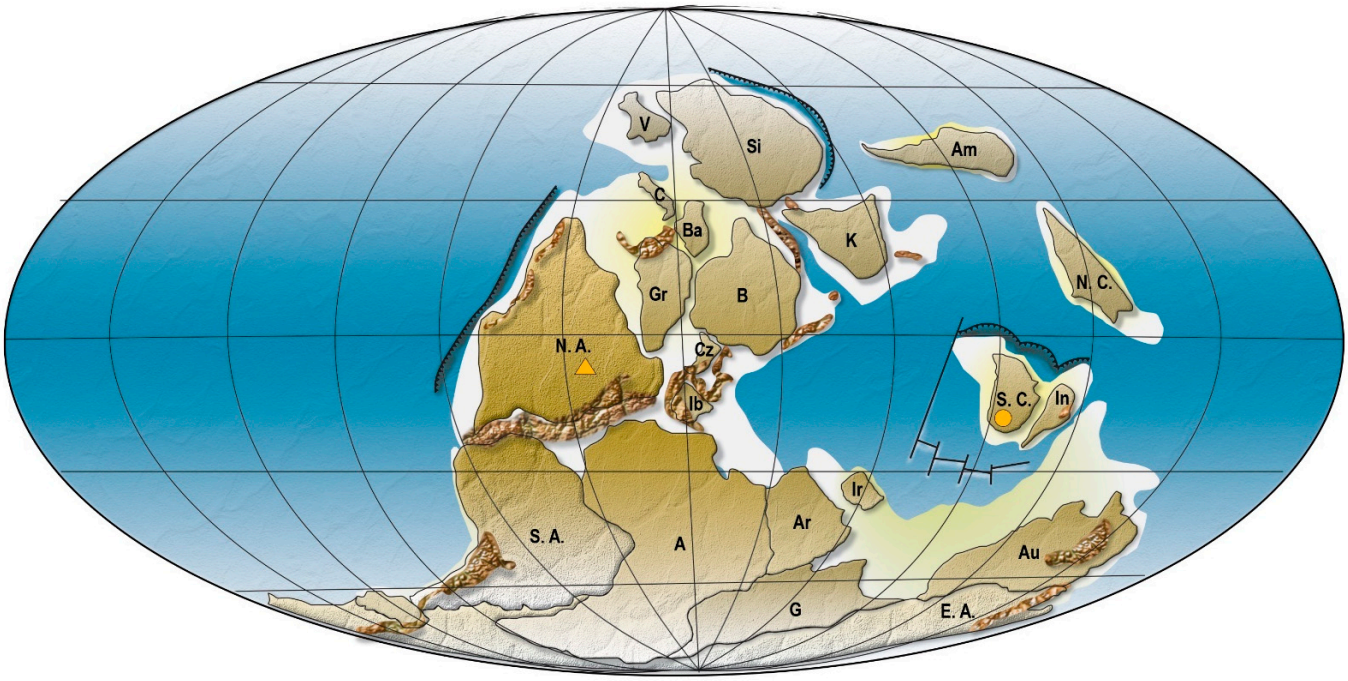


**Figure 7.** Paleogeographic map of continental masses during the Tournaisian showing the possible paleobiogeographic distribution of *Columnaodus* gen. nov. The yellow triangle represents the occurrence of *C. witzkei* sp. nov. and the yellow circle denotes the location of similar material. The depositional environments shown in Figure 2a would have occurred in the southern portion of the North American continental mass at this time. Abbreviations: A, Africa; Am, Amuria; Ar, Arabia; Au, Australia; B, Baltica; Ba, Barentsia; C, Chukotka; Cz, Czechia; E. A., East Antarctica; G, Gondwana; Gr, Greenland; Ib, Iberia; In, Indochina; Ir, Iran; K, Kazakhstan; N. A., North America; N. C., North China; S. A., South America; S C., South China; Si, Siberia; V, Verkhoyansk. The placement of the major tectonic plates is a composite of Golonka and Gawędo (2012), Golonka (2011), and Scotese (2001) [68–70].

**Supplementary Materials:** The following are available online at https://www.mdpi.com/article/10.3390/d16050276/s1.

**Author Contributions:** Conceptualization, C.C.; methodology, C.C., R.S. and L.F.; Software, D.A.C.; formal analysis, D.C., M.H., R.S., D.P. and D.A.C.; investigation, D.C., M.H., R.S., D.P. and D.A.C.; resources, D.C., C.C., L.F., R.S., D.P. and D.A.C.; data curation, D.C., C.C., L.F., R.S., D.P. and D.A.C.; writing-original draft preparation, M.H., D.C. and R.S.; writing-review and editing, D.C., C.C., R.S., L.F., D.P., D.A.C. and S.J.; visualization, C.C., L.F. and D.A.C.; project administration, C.C. and S.J. All authors have read and agreed to the published version of the manuscript.

**Funding:** This research received no external funding.

**Institutional Review Board Statement:** Not applicable.

**Data Availability Statement:** The Supplementary Information contains a list of chondrichthyan species.

**Acknowledgments:** We thank Donald Smith and the Cessford Construction Company for allowing us to collect samples from their quarries, and Michael Ginter for helping us recognize the potential new genus and species. Hoenig would also like to thank friends and family who have encouraged and supported him throughout the thesis project which served as the inspiration for this work. The editorial comments provided by three reviewers helped to improve an earlier version of this work.

**Conflicts of Interest:** The authors declare no conflict of interest.

## References

1. Witzke, B.J.; McKay, R.M.; Bunker, B.J.; Woodson, F.J. Stratigraphy and paleoenvironments of Mississippian strata in Keokuk and Washington Counties, southeast Iowa. In *Guidebook Series, No. 10*; Iowa Department of Natural Resources: Des Moines, IA, USA, 1990; p. 106. Available online: https://publications.iowa.gov/id/eprint/25602 (accessed on 1 April 2019).
2. Newberry, J.S.; Worthen, A.H. Descriptions of new species of vertebrates, mainly from the Sub-Carboniferous limestone and coal measures of Illinois. In *Geological Survey of Illinois*; Worthen, A.H., Ed.; State Journal Steam Press: Springfield, IL, USA, 1866; Volume 2, pp. 9–134. [CrossRef]
3. Wachsmuth, C.; Springer, F. Transition forms in crinoids, and description of five new species. *Proc. Acad. Nat. Sci. Phila.* **1878**, *30*, 224–266. Available online: https://www.jstor.org/stable/4060405 (accessed on 1 April 2019).
4. Witzke, B.J.; Bunker, B.J. Relative sea-level changes during Middle Ordovician through Mississippian deposition in the Iowa area, North American Craton. In *Paleozoic Sequence Stratigraphy; Views from the North American Craton*; Witzke, B.J., Ludvigson, G.A., Day, J., Eds.; Geological Society of America Special Papers; Geological Society of America: McLean, VA, USA, 1996; Volume 306, pp. 307–330. [CrossRef]
5. Leidy, J. Descriptions of the remains of fishes from the Carboniferous Limestone of Illinois and Missouri. *Trans. Am. Philos. Soc* **1860**, *11*, 87–90. [CrossRef]
6. Newberry, J.S.; Worthen, A.H. Descriptions of fossil vertebrates. In *Geological Survey of Illinois*; Worthen, A.H., Ed.; State Journal Steam Press: Springfield, IL, USA, 1870; Volume 4, pp. 343–374. [CrossRef]
7. St. John, O.; Worthen, A.H. Descriptions of fossil fishes. In *Geological Survey of Illinois*; Worthen, A.H., Ed.; State Journal Steam Press: Springfield, IL, USA, 1875; Volume 6, pp. 245–488. [CrossRef]
8. Newberry, J.S. Personal letter. In *Eighth, Ninth, and Tenth Annual Reports of the Geological Survey of Indiana, Made during the Years 1876-77-78*; Cox, E.T., Collett, J., Levette, G.M., Eds.; Indianapolis Journal Company: Indianapolis, IN, USA, 1879; Volumes 8–10, pp. 341–349.
9. St. John, O.; Worthen, A.H. Descriptions of fossil vertebrates. In *Geological Survey of Illinois*; Worthen, A.H., Ed.; State Journal Steam Press: Springfield, IL, USA, 1883; Volume 7, pp. 53–264. [CrossRef]
10. Newberry, J.S. New species and a new genus of American Palaeozoic fishes, together with notes on the genera *Oracanthus*, *Dactylodus*, *Polyrhizodus*, *Sandalodus*, *Deltodus*. *Trans. N. Y. Acad. Sci.* **1897**, *16*, 282–304.
11. Hay, O.P. On some changes in the names, generic and specific, of certain fossil fishes. *Am. Nat.* **1899**, *33*, 783–792. Available online: https://www.jstor.org/stable/2454274 (accessed on 1 April 2019). [CrossRef]
12. Branson, E.B. Notes on some Carboniferous Cochliodonts with descriptions of seven new species. *J. Geol.* **1905**, *13*, 20–34. Available online: https://www.jstor.org/stable/30066320 (accessed on 1 April 2019). [CrossRef]
13. Ginter, M.; Duffin, C.; Hampe, O. *Handbook of Paleoichthyology: Chondrichthyes IV*; Verlag Dr. Friedrich Pfeil: München, Germany, 2010; Volume 3D, pp. 1–168.
14. Newberry, J.S. The Paleozoic fishes of North America. In *Monographs of the United States Geological Survey*; U.S. Government Printing Office: Washington, DC, USA, 1889; Volume 16, p. 340. [CrossRef]
15. Hodnett, J.-P.M.; Elliott, D.K.; Olson, T.J. A new basal hybodont (Chondrichthyes, Hybodontiformes) from the Middle Permian (Roadian) Kaibab Formation, of northern Arizona. In *The Carboniferous-Permian Transition*; Lucas, S.G., DiMichele, W.A., Barrick, J.E., Schneider, J.W., Spielmann, J.A., Eds.; New Mexico Museum of Natural History and Science: Albuquerque, NM, USA, 2013; Bulletin 60; pp. 103–108.
16. Harris, S.E.; Parker, M.C. Stratigraphy of the Osage series in Southeastern Iowa. In *Report of Investigations 1*; Iowa Geological Survey: Iowa, IA, USA, 1964; pp. 1–52. [CrossRef]
17. Mamet, B.L. Taxonomic note on Carboniferous Endothyracea. *J. Foramin. Res.* **1974**, *4*, 200–204. [CrossRef]
18. Mamet, B.L. Foraminiferal zonation of the Lower Carboniferous: Methods and stratigraphic implications. In *Concepts and Methods of Biostratigraphy*; Kauffman, E.G., Hazel, J.E., Eds.; Dowden, Hutchinson, and Ross: Stroudsburg, PA, USA, 1977; pp. 445–462.
19. Chauff, K.M. Multielement conodont species from the Osagean (Early Mississippian) Burlington Carbonate Shelf, Midcontinent North America, and the Chappel Limestone of Texas. Ph.D. Dissertation, University of Iowa, Iowa City, IA, USA, 1978.
20. Lane, H.R. The Burlington Shelf (Mississippian, north-central United States). *Geol. Palaeontol.* **1978**, *12*, 165–176.
21. Lane, H.R.; Sandberg, C.A.; Ziegler, W. Taxonomy and phylogeny of some Lower Carboniferous conodonts and preliminary standard post-*Siphonodella* zonation. *Geol. Palaeontol.* **1980**, *14*, 117–164.
22. Chauff, K.M. Multielement conodont species and an ecological interpretation of the Lower Osagean (Lower Carboniferous) conodont zonation from Midcontinent North America. *Micropaleontology* **1983**, *29*, 404–429. Available online: https://www.jstor.org/stable/1485517 (accessed on 1 April 2019). [CrossRef]

23. Lane, H.R.; Brenckle, P.L. Type Mississippian subdivisions and biostratigraphic succession. In *Stratigraphy and Biostratigraphy of the Mississippian Subsystem (Carboniferous System) in Its Type Region, the Mississippi River Valley of Illinois, Missouri, and Iowa*; Heckel, P.H., Ed.; Illinois State Geological Survey: Champaign, IL, USA, 2005; Guidebook 34; pp. 76–105.
24. Cohen, K.M.; Finney, S.C.; Gibbard, P.L.; Fan, J.-X. The ICS International Chronostratigraphic Chart, Episodes 36. 2013. Updated. pp. 199–204. Available online: http://www.stratigraphy.org/ICSchart/ChronostratChart2023-06.pdf (accessed on 1 April 2019).
25. Torsvik, T.H.; Cocks, L.R.M. *Earth History and Palaeogeography*; Cambridge University Press: Cambridge, UK, 2017; 317p. [CrossRef]
26. Lane, H.R.; De Keyser, T.L. Paleogeography of the late Early Mississippian (Tournaisian 3) in the central and southwestern United States. In *Paleozoic Paleogeography of the West-Central United States: Rocky Mountain Symposium 1*; Fouch, T.D., Magathan, E.R., Eds.; Society of Economic Paleontologists and Mineralogists, Rocky Mountain Section: Fort Collins, CO, USA, 1980; pp. 149–162.
27. Ross, C.A.; Ross, J.R.P. Late Paleozoic sea levels and depositional sequences. *Geol. Fac. Publ.* **1987**, *61*, 137–149. Available online: https://cedar.wwu.edu/geology_facpubs (accessed on 1 April 2019).
28. Harris, D.C. Carbonate Cement Stratigraphy and Diagenesis of the Burlington Limestone (Miss.), South-East Iowa and West Illinois. Master's Thesis, State University of New York at Stony Brook, Stony Brook, NY, USA, 1982.
29. Van Tuyl, F.M. The stratigraphy of the Mississippian formations of Iowa. *Iowa Geol. Surv. Annu. Rep.* **1923**, *30*, 33–360. [CrossRef]
30. Cander, H.S.; Kaufman, J.; Daniels, L.D.; Meyers, W.J. Regional dolomitization of shelf carbonates in the Burlington-Keokuk Formation (Mississippian), Illinois and Missouri: Constraints from cathodoluminescent zonal stratigraphy. In *Sedimentology and Geochemistry of Dolostones*; Shukla, V., Baker, P.A., Eds.; SEPM Society for Sedimentary Geology: Claremore, OK, USA, 1988; Volume 43, pp. 129–144. [CrossRef]
31. Banner, J.L.; Hanson, G.N.; Meyers, W.J. Rare earth element and Nd isotopic variations in regionally extensive dolomites from the Burlington-Keokuk Formation (Mississippian): Implications for REE mobility during carbonate diagenesis. *J. Sediment. Petrol.* **1988**, *58*, 415–432. [CrossRef]
32. Reif, W.E. Muschelkalk/Keuper bone-beds (Middle-Triassic, SW-Germany)-storm condensation in a regressive cycle. In *Cyclic and Event Stratification*; Einsele, G., Seilacher, A., Eds.; Springer: Berlin/Heidelberg, Germany, 1982; pp. 299–325. [CrossRef]
33. Macquaker, J.H.S. Palaeoenvironmental significance of 'bone-beds' in organic-rich mudstone successions: An example from the Upper Triassic of south-west Britain. *Zool. J. Linn. Soc-Lond.* **1994**, *112*, 285–308. [CrossRef]
34. Brett, C.E. Sequence stratigraphy, biostratigraphy, and taphonomy in shallow marine environments. *Palaios* **1995**, *10*, 597–616. [CrossRef]
35. Pyenson, N.D.; Irmis, R.B.; Lipps, J.H.; Barnes, L.G.; Mitchell, E.D., Jr.; McLeod, S.A. Origin of a widespread marine bonebed deposited during the middle Miocene Climatic Optimum. *Geology* **2009**, *37*, 519–522. [CrossRef]
36. Jeppsson, L.; Fredholm, D.; Mattiasson, B. Acetic acid and phosphatic fossils: A warning. *J. Paleontol.* **1985**, *59*, 952–956. Available online: https://www.jstor.org/stable/1304939 (accessed on 4 October 2023).
37. Jeppsson, L.; Anehus, R. A buffered formic acid technique for conodont extraction. *J. Paleontol.* **1995**, *69*, 790–794. Available online: https://www.jstor.org/stable/1306313 (accessed on 4 October 2023). [CrossRef]
38. Jeppsson, L.; Anehus, R.; Fredholm, D. The optimal acetate buffered acetic acid technique for extracting phosphatic fossils. *J. Paleontol.* **1999**, *73*, 964–972. Available online: https://www.jstor.org/stable/1306854 (accessed on 4 October 2023). [CrossRef]
39. Huxley, T. *A Manual of the Anatomy of Vertebrated Animals*; D. Appleton and Co.: New York, NY, USA, 1880; pp. 1–431.
40. Bonaparte, C.L.J.L. Selachorum tabula analytica. Systema Icthyologicum. *Mem. Soc. Neuchatel. Sci. Nat.* **1838**, *2*, 1–16.
41. Hay, O.P. Bibliography and catalogue of the fossil Vertebrata of North America. In *Bulletin of the United States Geological Survey*; US Government Printing Office: Washington, DC, USA, 1902; No. 179; pp. 1–868.
42. Maisey, J.G. The interrelationships of phalacanthous selachians. *Neues Jahr. Geol. Palaeontol. Monatsh.* **1975**, *9*, 563–567.
43. Owen, R. *Lectures on the Comparative Anatomy and Physiology of the Vertebrate Animals: Delivered at the Royal College of Surgeons of England, in 1844 and 1846. Part 1 Fishes*; Longman, Brown, Green, and Longmans: London, UK, 1846; pp. 1–308. [CrossRef]
44. Enault, S.; Guinot, G.; Koot, M.B.; Cuny, G. Chondrichthyan tooth enameloid: Past, present, and future. *Zool. J. Linn. Soc-Lond.* **2015**, *174*, 549–570. [CrossRef]
45. Ivanov, A.O.; Duffin, C.J.; Naugolnykh, S.V. A new euselachian shark from the early Permian of the Middle Urals, Russia. *Acta Palaeontol. Pol.* **2017**, *62*, 289–298. [CrossRef]
46. Kriwet, J. Late Jurassic selachians (Chondrichthyes: Hybodontiformes, Neoselachii) from southern Germany: Re-evaluation on taxonomy and diversity. *Zitteliana A* **2004**, *44*, 67–95.
47. Rees, J. Interrelationships of Mesozoic hybodont sharks as indicated by dental morphology—Preliminary results. *Acta Geol. Pol.* **2002**, *58*, 217–221.
48. Wen, W.; Zhang, Z.; Kriwet, J.; Hu, S.; Zhour, C.; Huang, J.; Cui, X.; Min, X.; Benton, M.J. First occurrence of hybodontid teeth in the Louping Biota (Middle Triassic, Anisian) and recovery of the marine ecosystem after the end-Permian mass extinction. *Palaeogeogr. Palaeoclimatol. Palaeoecol.* **2023**, *617*, 111471. [CrossRef]
49. Dick, R.F. On the Carboniferous shark *Tristychius arcuatus* Agassiz from Scotland. *Earth Environ. Sci. Trans. R. Soc.* **1978**, *70*, 63–109. [CrossRef]
50. Maisch, M.W.; Matzke, A.T. A new hybodontid shark (Chondrichthyes, Hybodontiformes) from the Lower Jurassic Posidonienschiefer Formation of Dotternhause, SW Germany. *Neues Jahrb. Geol. Paläontologie Abh.* **2016**, *280*, 241–257. [CrossRef]

51. Murry, P.A.; Kirby, R.E. A new hybodont shark from the Chinle and Bull Canyon Formations, Arizona, Utah, and New Mexico. In *Upper Triassic Stratigraphy and Paleontology*; Heckert, A.B., Lucas, S.G., Eds.; New Mexico Museum of Natural History: Albuquerque, NM, USA, 2002; Bulletin 21; pp. 87–106.
52. Fischer, J.; Schneider, J.W.; Ronchi, A. New hybondontoid shark from the Permocarboniferous (Gzhelian-Asselian) of Guardia Pisano (Sardinia, Italy). *Acta Palaeontol. Pol.* **2010**, *55*, 241–264. [CrossRef]
53. Wang, N.Z.; Zhang, X.; Zhu, M.; Zhao, W.J. A new articulated hybodontoid from Late Permian of northwestern China. *Acta Zool. Stockholm* **2009**, *90*, 159–170. [CrossRef]
54. Bhat, M.S.; Ray, S.; Datta, P.M. A new hybodont shark (Chondrichthyes, Elasmobranchii) from the Upper Triassic Tiki Formation of India with remarks on its dental histology and biostratigraphy. *J. Paleontol.* **2018**, *92*, 221–239. [CrossRef]
55. Casier, E. Contributions à l'étude des poissons fossiles de la Belgique. XII Sélaciens et Holocéphales sinémuriens de la province de Luxembourg. *Bull. R. Belg. Inst. Nat. Sci.* **1959**, *35*, 1–35.
56. Herman, J. Les Sélaciens des terrains néocrétacés et paléocènes de Belgique et des contrées limitrophes. Eléments d'une biostratigraphie intercontinentale. *Mémoires Pour Serv. L'explication Cart. Géologiques Minières Belg.* **1977**, *15*, 1–401.
57. Glickman, L.S. Class Chondrichthyes, Subclass Elasmobranchii. In *Fundamental of Paleontology*; Obruchev, D.V., Ed.; Nauka SSSR: Moscow-Leningrad, Russia, 1964; Volume 11, pp. 196–237.
58. Maisey, J.G. *Hamiltonichthys mapesi, g. and sp. nov., (Chondrichthyes, Elasmobranchii) from the Upper Pennsylvanian of Kansas*; American Museum of Natural History: New York, NY, USA, 1989; No. 2931; p. 42.
59. Coates, M.I.; Gess, R.W. A new reconstruction of Onychoselache traquairi, comments on early chondrichtyan pectoral girdles and hybodontiform phylogeny. *Palaeontology* **2007**, *50*, 1421–1446. [CrossRef]
60. Johnson, G.D. Hybodontoidei (Chondrichthyes) from the Wichita-Albany Group (Early Permian) of Texas. *J. Vertebr. Paleontol.* **1981**, *1*, 1–41. Available online: https://www.jstor.org/stable/4522833 (accessed on 4 October 2023). [CrossRef]
61. Dick, R.F.; Maisey, J.G. Scottish Lower Carboniferous shark Onychoselache traquairi. *Palaeontology* **1980**, *23*, 363–374.
62. Hairapetian, V.; Ginter, M. Famennian chondrichthyan remains from the Chahriseh section, central Iran. *Acta Geol. Pol.* **2009**, *59*, 173–200.
63. Zangerl, R. New chondrichthyes from the Mazon Creek fauna (Pennsylvanian) of Illinois. In *Mazon Creek Fossils*; Nitecki, M.H., Ed.; Academic Press: New York, NY, USA, 1979; pp. 449–500.
64. Duffin, C.J. Revision of the hybodont selachian genus *Lissodus* Brough (1935). *Palaontographica Abt. A* **1985**, *188*, 105–152.
65. Klug, S.; Tutken, T.; Wings, O.; Pfretzschner, H.-U.; Martin, T. A Late Jurassic freshwater shark assemblage (Chondrichthyes, Hybodontiformes) from the southern Junggar Basin, Xinjiang, Northwest China. *Palaeobiology Palaeoenvironment* **2010**, *90*, 241–257. [CrossRef]
66. Ginter, M.; Sun, Y. Chondrichthyan remains from the Lower Carboniferous of Muhua, southern China. *Acta Palaeontol. Pol.* **2007**, *52*, 705–727.
67. Baumiller, T.K.; Gahn, F.J. Predation on Crinoids. In *Predator-Prey Interactions in the Fossil Record*; Kelley, P.H., Kowalewski, M., Hansen, T.A., Eds.; Springer: Boston, MA, USA, 2003; pp. 263–278. [CrossRef]
68. Golonka, J.; Gawęda, A. Plate tectonic evolution of the southern margin of Laurussia in the Paleozoic. In *Tectonics: Recent Advances*; Sharkov, E., Ed.; InTech: Rijeka, Croatia, 2012; pp. 261–282.
69. Golonka, J. Chapter 6 Phanerozoic palaeoenvironment and palaeolithofacies maps of the Arctic region. In *Arctic Petroleum Geology*; Spencer, A.M., Embry, A.F., Gautier, D.L., Stoupakova, A.V., Sørensen, K., Eds.; Geological Society, London, Memoirs: London, UK, 2011; Volume 35, pp. 79–129.
70. Scotese, C.R. *Atlas of Earth History*; PALEOMAP Project: Arlington, TX, USA, 2001; pp. 1–58.